The characteristic equation of an oscillating viscoelastic drop

Dino Zrnić*, Günter Brenn
Institute of Fluid Mechanics and Heat Transfer, Graz University of Technology 8010 Graz, Austria
*Corresponding author: dzrnic@tugraz.at

Abstract
A study of axisymmetric shape oscillations of a viscoelastic drop in a vacuum using the method of weakly nonlinear analysis is conducted. The work is carried out due to the relevance of the analysis for transport processes across the drop surface and due to fundamental interest. The Oldroyd-B model is used for the characterization of the rheological liquid behaviour. The method applied yields a set of governing equations, boundary and initial conditions for different orders of approximation. In the present paper, the first-order equations and solutions with the characteristic equation for the viscoelastic drop are presented. The characteristic equation yields an infinite number of roots [5], which determine the time dependency in the higher-order solutions. The number of selected roots defines the number of initial conditions needed for the corresponding order of approximation. The solutions of the characteristic equation are selected according to experiments conducted on an acoustically levitated drop. Experimental data are obtained by measuring damping factor and oscillation frequency based on free damped shape oscillations of viscoelastic aqueous polymer solution drops.

Keywords
Drop shape oscillations; weakly nonlinear analysis; viscoelastic behaviour; Oldroyd-B; complex angular frequency

Introduction

For more than 140 years, shape oscillations of drops have been a subject of scientific investigations for fundamental interest and for their relevance for transport processes. The drop surface deformations against the spherical state raise the surface area and induce motions inside and outside the liquid drop. The interaction with the ambient gas phase influences gradients of velocity, temperature and species concentration, which determine the transport of momentum, heat and mass across the drop surface. In the appendix to his paper on the capillary phenomena of jets [12], Rayleigh presented an analysis of linear shape oscillations of an inviscid drop in a vacuum around a spherical equilibrium state. One result is the equation for the angular frequency of oscillation of the drop deformed according to a mode m assuming natural values $m = 2, 3, 4, \ldots$, which count the number of lobes along the drop surface. In [7, 8], Lamb generalised Rayleigh's result by accounting for the drop viscosity and the density of the ambient medium. The threshold Ohnesorge number $Oh = \mu/(\sigma a \rho)^{1/2}$ of the drop for the onset of aperiodic motion was proposed.
Chandrasekhar developed the characteristic equation analysing small shape oscillations of a viscous, self-gravitating globe in a vacuum [4]. In [10], the analysis of linear drop shape oscillations was further generalised by account for both the viscous and the inertial influences from the ambient medium hosting the viscous oscillating drop. Prosperetti studied the important aspect of initiation of the oscillations. In his paper [11], he analysed the drop shape oscillations as the solution of an initial-value problem and showed that the normal-mode approach may miss the fact that, in a range of Ohnesorge numbers, oscillations starting aperiodically may turn into periodic with ongoing time. The most important results from the here cited highlight papers are the angular frequency and damping rate of the oscillations, and the time-dependent shapes of the oscillating drops.

First computational investigations of nonlinear drop shape oscillations with large amplitudes are due to [6] and [1]. Both Foote and Alonso used the marker-and-cell finite-difference technique for numerically simulating the time-dependent free-surface flows with weak influence from the liquid viscosity. First experimental studies of large-amplitude shape oscillations of drops in an immiscible host liquid and of levitated free liquid drops in air are due to [16], who showed the frequency decrease with increasing drop deformation and an asymmetry of the times spent in the prolate and oblate shapes of the two-lobed oscillation mode [17]. One of the first analyses of small-amplitude axisymmetric shape deformations of a viscoelastic liquid drop in microgravity is [5]. Asymptotic analyses in the low- and high-viscosity limits and for low, moderate and large elasticities are performed. They established the characteristic equation for a viscoelastic drop and found that the equation gives an infinite number of roots, depending critically on the values of the relaxation and retardation times, as well as the surface tension.
The aim of the work in progress reported here is to extend the above investigations to a nonlinear description of shape oscillations of a viscoelastic drop. We report the theoretical approach which is analogous to the recently published weakly nonlinear stability analysis of a Newtonian liquid drop [18]. The present paper shows the method used for solving the characteristic equation and properly accounting for the solutions. A combination with experiments on an individual acoustically levitated oscillating drop is the key. In these experiments, an individual drop of the test liquid is positioned in the pressure field of the acoustic levitator. Modulation of the sound pressure drives the drop to shape oscillations of a given mode, for which damping factor and oscillation frequency are measured.

Theory - formulation of the problem

Nonlinear shape oscillations of a viscoelastic liquid drop are studied. The drop shapes, as sketched in figure 1, are axisymmetric, and the motion is represented in spherical coordinates to account for the geometry. The liquid is treated as incompressible, and its viscoelastic behaviour upon rates of deformation is represented by the Oldroyd-B model. Analysing the drop motion in a vacuum, the dynamic influence from an ambient medium is neglected. Body forces are not accounted for, since the Froude number is large.
The equations of motion with their initial and boundary conditions are non-dimensionalized with the undeformed drop radius a, the capillary time scale $(\rho a^3/\sigma)^{1/2}$, the capillary pressure σ/a and the viscous stress $\mu_0(\sigma/\rho a^3)^{1/2}$ for length, time, pressure and extra stress, respectively. Here, ρ is the liquid density, σ the vacuum-liquid interfacial tension and μ_0 the zero-shear viscosity of the drop liquid. The drop surface is described as the place where $r_s(\theta,t) = 1+\eta(\theta,t)$, with the non-dimensional deformation η against the undisturbed spherical shape (cf. Figure 1). For the problem at hand, the equation of continuity and the two components of the momentum equation in the radial and polar angular directions, (r) and (θ), read

$$\frac{1}{r^2}\frac{\partial}{\partial r}\left(r^2 u_r\right) + \frac{1}{r\sin\theta}\frac{\partial}{\partial\theta}\left(u_\theta \sin\theta\right) = 0\,, \tag{1}$$

$$\begin{aligned}\frac{\partial u_r}{\partial t} + u_r\frac{\partial u_r}{\partial r} &+ \frac{u_\theta}{r}\frac{\partial u_r}{\partial\theta} - \frac{u_\theta^2}{r} = -\frac{\partial p}{\partial r} \\ &+ Oh_0\left[\frac{1}{r^2}\frac{\partial}{\partial r}\left(r^2\tau_{rr}\right) + \frac{1}{r\sin\theta}\frac{\partial}{\partial\theta}\left(\tau_{r\theta}\sin\theta\right) - \frac{\tau_{\theta\theta}+\tau_{\phi\phi}}{r}\right]\,,\end{aligned} \tag{2}$$

$$\begin{aligned}\frac{\partial u_\theta}{\partial t} + u_r\frac{\partial u_\theta}{\partial r} &+ \frac{u_\theta}{r}\frac{\partial u_\theta}{\partial\theta} + \frac{u_r u_\theta}{r} = -\frac{1}{r}\frac{\partial p}{\partial\theta} + \\ &+ Oh_0\left[\frac{1}{r^2}\frac{\partial}{\partial r}\left(r^2\tau_{r\theta}\right) + \frac{1}{r\sin\theta}\frac{\partial}{\partial\theta}\left(\tau_{\theta\theta}\sin\theta\right) + \frac{\tau_{r\theta}}{r} - \frac{\cot\theta}{r}\tau_{\phi\phi}\right]\,,\end{aligned} \tag{3}$$

where $Oh_0 = \mu_0/(\sigma a\rho)^{1/2}$ is the Ohnesorge number, the characteristic dimensionless parameter measuring viscosity influences. The viscoelastic liquid material is characterised by the

nondimensional rheological constitutive equation (RCE) of the Oldroyd-B fluid

$$\boldsymbol{\tau} + De_1 \overset{\triangledown}{\boldsymbol{\tau}} = 2\left(\boldsymbol{D} + De_2 \overset{\triangledown}{\boldsymbol{D}}\right) , \tag{4}$$

where $\boldsymbol{\tau}$ and $\boldsymbol{D}$ are the extra-stress and rate-of-deformation tensors, respectively, the latter defined with the velocity gradient tensor $\vec{\nabla}\vec{v}$ as

$$\boldsymbol{D} = \frac{1}{2}\left(\vec{\nabla}\vec{v} + \vec{\nabla}\vec{v}^T\right) . \tag{5}$$

The Deborah numbers $De_1 = \lambda_1(\sigma/\rho a^3)^{1/2}$ and $De_2 = \lambda_2(\sigma/\rho a^3)^{1/2}$ represent the nondimensional stress relaxation and deformation retardation times of the liquid, respectively. The upper-convected derivative $\overset{\triangledown}{\boldsymbol{A}}$ of a tensor $\boldsymbol{A}$ is given as

$$\overset{\triangledown}{\boldsymbol{A}} = \frac{d\boldsymbol{A}}{dt} - \vec{\nabla}\vec{v}\cdot\boldsymbol{A} - \boldsymbol{A}\cdot\vec{\nabla}\vec{v}^T , \tag{6}$$

where $d\boldsymbol{A}/dt$ is the material derivative.
The above set of equations is solved subject to initial and boundary conditions. The kinematic boundary condition states that the material rate of deformation of the drop surface equals the radial velocity component at the place of the deformed surface, i.e.,

$$u_r = \frac{d\eta}{dt} = \frac{\partial\eta}{\partial t} + \frac{u_\theta}{r}\frac{\partial\eta}{\partial\theta} \quad \text{at} \quad r = 1+\eta. \tag{7}$$

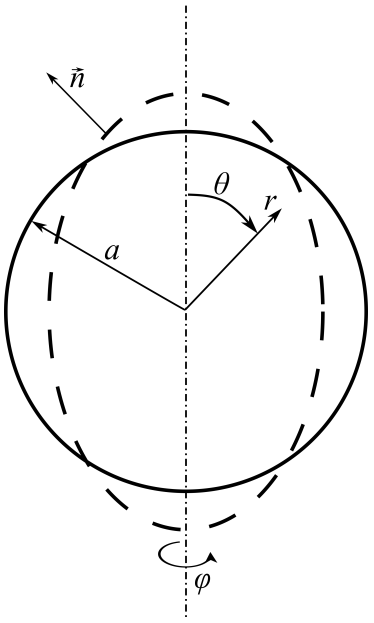

Figure 1. Geometry of a liquid drop under deformation at mode 2 [17].

The first dynamic boundary condition states that the shear stress at the drop surface is zero, since we assume that, in a vacuum, the dynamic viscosity is negligible, so that momentum cannot be transferred across the drop boundary at an appreciable rate. The second dynamic boundary condition states that the stress normal to the drop surface, composed from the flow-induced pressure and the viscoelastic normal stress, differs across the interface by the stress due to the surface tension. The zero-shear stress boundary condition reads

$$(\vec{n}\cdot\tau)\times\vec{n} = \vec{0} \quad \text{at} \quad r = 1+\eta, \tag{8}$$

where the outward unit normal vector $\vec{n}$ is given as

$$\vec{n} = \frac{1}{|\vec{\nabla}F|}\vec{\nabla}F \quad \text{with} \quad F = r - 1 - \eta(t,\theta) = 0, \tag{9}$$

and the extra stress tensor in (8) is the one for the incompressible Oldroyd-B fluid. The corresponding normal stress boundary condition reads

$$-p + Oh_0\,(\vec{n}\cdot\boldsymbol{\tau})\cdot\vec{n} + \left(\vec{\nabla}\cdot\vec{n}\right) = 0 \quad \text{at} \quad r = 1+\eta. \tag{10}$$

We obtain the divergence of the normal unit vector on the drop surface in this equation as

$$\left(\vec{\nabla}\cdot\vec{n}\right) = \frac{1}{r}\frac{2+3\left(\frac{1}{r}\frac{\partial\eta}{\partial\theta}\right)^2}{\left[1+\left(\frac{1}{r}\frac{\partial\eta}{\partial\theta}\right)^2\right]^{3/2}} - \frac{1}{r^2\sin\theta}\frac{\partial}{\partial\theta}\left[\frac{\frac{\partial\eta}{\partial\theta}}{\left(1+\left(\frac{1}{r}\frac{\partial\eta}{\partial\theta}\right)^2\right)^{1/2}}\sin\theta\right] \quad \text{at} \quad r = 1+\eta. \tag{11}$$

For analyzing these equations in a weakly nonlinear form, the two velocity components, the pressure and the extra stress tensor in the flow field, as well as the deformed interface shape,

are expanded in power series with respect to a small deformation parameter η_0. We therefore formulate the expansions of the flow field properties, for example u_r and p, as

$$u_r = u_{r1}\eta_0 + u_{r2}\eta_0^2 + u_{r3}\eta_0^3 \dots , \tag{12}$$

$$p = p_0 + p_1\eta_0 + p_2\eta_0^2 + p_3\eta_0^3 \dots , \tag{13}$$

where η, $\boldsymbol{\tau}$ and $\boldsymbol{D}$ are expanded in the same manner as u_r. The deformation parameter η_0 must be small for convergence of these series expansions. The boundary conditions are satisfied on the deformed drop surface using Taylor expansions, such as, for example for u_r,

$$u_r|_{r=1+\eta} = u_r|_{r=1} + \left.\frac{\partial u_r}{\partial r}\right|_{r=1} \eta + \dots , \tag{14}$$

where p and $\boldsymbol{\tau}$ are expanded in the same manner. Substituting these approaches into the equations of motion (1) - (3), into the RCE (4) and into the boundary conditions (7), (8) and (10), and representing the flow properties and their derivatives as given in (12) through (14), we obtain sets of first-, second- and third-order equations of motion, with the boundary conditions, consisting of all the terms with the deformation parameter η_0 to the first, second and third powers, respectively [17, 18].

The drop motion is induced by an initially imposed surface deformation against the spherical shape. The initial deformation is governed by a Legendre polynomial of degree m with the amplitude η_0, and the surface is taken to be at rest initially. Calculation of the volume of the deformed drop leads to the expression

$$\begin{aligned} r_s(\theta,0) &= 1+\eta(\theta,0) \\ &= \left(1+\frac{3\eta_0^2}{2m+1}+\frac{1}{2}\eta_0^3\int_{-1}^{1} P_m(\cos\theta)^3 d(\cos\theta)\right)^{-1/3} + \eta_0 P_m(\cos\theta) \\ &= 1+\eta_0 P_m(\cos\theta) - \eta_0^2\frac{1}{2m+1} - \frac{\eta_0^3}{6}\int_{-1}^{1} P_m(\cos\theta)^3 d(\cos\theta) \mp \dots , \end{aligned} \tag{15}$$

for the initial non-dimensional drop shape. The factor in front of η_0 to the respective power is the term for the corresponding order of approximation needed that the surface shape represents the correct drop volume. Moreover, for the development of the solutions of the problem of drop shape oscillations, the angular frequencies corresponding to the oscillation modes zero and one are required, which, in contrast to all the other modes, do not follow as a solution of the characteristic equation of the drop. To overcome this problem, use will be made of the requirement that the centre of mass of the drop remains at its initial position

$$z_m = \frac{\pi}{2V}\int_{-1}^{1}\left[1+4\eta_0\eta_1+\eta_0^2\left(6\eta_1^2+4\eta_2\right)+\eta_0^3\left(4\eta_1^3+12\eta_1\eta_2+4\eta_3\right)+\dots\right] x dx , \tag{16}$$

at all times. Physically, this is justified because there is no resultant force making the drop move [18]. Due to limitation in the paper length and interest in the first-order equations and solutions, the higher orders of approximation will be presented elsewhere [19].

First-order equations

To obtain the first-order equations with their boundary and initial conditions, the above series expansions are introduced into the respective equations, and all the terms with the parameter η_0 to the first power are collected. The first-order continuity and momentum equations read

$$\frac{1}{r^2}\frac{\partial}{\partial r}\left(r^2 u_{r1}\right) + \frac{1}{r\sin\theta}\frac{\partial}{\partial\theta}\left(u_{\theta 1}\sin\theta\right) = 0 , \tag{17}$$

$$\begin{aligned} \frac{\partial u_{r1}}{\partial t} &= -\frac{\partial p_1}{\partial r} + \\ &+ Oh_0\left[\frac{1}{r^2}\frac{\partial}{\partial r}\left(r^2\tau_{rr1}\right)+\frac{1}{r\sin\theta}\frac{\partial}{\partial\theta}\left(\tau_{r\theta 1}\sin\theta\right)-\frac{\tau_{\theta\theta 1}+\tau_{\phi\phi 1}}{r}\right] , \end{aligned} \tag{18}$$

$$\frac{\partial u_{\theta 1}}{\partial t} = -\frac{1}{r}\frac{\partial p_1}{\partial \theta} + \\ + Oh_0\left[\frac{1}{r^2}\frac{\partial}{\partial r}\left(r^2\tau_{r\theta 1}\right) + \frac{1}{r\sin\theta}\frac{\partial}{\partial\theta}\left(\tau_{\theta\theta 1}\sin\theta\right) + \frac{\tau_{r\theta 1}}{r} - \frac{\cot\theta}{r}\tau_{\phi\phi 1}\right] . \tag{19}$$

The RCE of first order becomes

$$\boldsymbol{\tau}_1 + De_1\frac{\partial\boldsymbol{\tau}_1}{\partial t} = 2\left(\boldsymbol{D}_1 + De_2\frac{\partial\boldsymbol{D}_1}{\partial t}\right) . \tag{20}$$

As the boundary conditions of first order, to be satisfied at $r = 1$, we obtain

$$u_{r1} = \frac{\partial\eta_1}{\partial t} , \quad \tau_{r\theta 1} = 0 \quad \text{and} \quad -p_1 + Oh_0\tau_{rr1} - \left(2\eta_1 + \frac{\partial\eta_1}{\partial\theta}\cot\theta + \frac{\partial^2\eta_1}{\partial\theta^2}\right) = 0 , \tag{21}$$

respectively. Furthermore, the initial conditions of first order are

$$\eta_1(\theta, 0) = P_m(\cos\theta) , \quad \frac{\partial\eta_1}{\partial t}(\theta, 0) = 0 . \tag{22}$$

The first initial condition determines the initial shape of the deformed drop, which is given by a Legendre polynomial of order m, and the second one states that the drop surface is initially at rest. We have thus completed the first-order equations and conditions, and therefore we can proceed with the derivation of the solution, which is shown in the following subsection.

First-order solutions

The first-order equations describe the linear problem. Since only two-dimensional flow fields are investigated, we apply the method of the Stokesian streamfunction for determining the first-order velocity and pressure fields [18]. The streamfunction $\psi(r, \theta, t)$ is defined by its relations to the two velocity components u_{r1} and $u_{\theta 1}$ as [3]

$$u_{r1} = -\frac{1}{r^2\sin\theta}\frac{\partial\psi}{\partial\theta} \quad \text{and} \quad u_{\theta 1} = \frac{1}{r\sin\theta}\frac{\partial\psi}{\partial r} . \tag{23}$$

These first-order velocity components satisfy the continuity equation identically.

The first-order drop surface deformation is governed by the Legendre polynomial of the initial deformation. The shape is therefore sought in the form

$$\eta_1(\theta, t) = \hat{\eta}_1 P_m(\cos\theta)e^{-\alpha_m t} , \tag{24}$$

with the first-order initial surface amplitude $\hat{\eta}_1$ and the first-order complex angular frequency α_m for the deformation mode m.

For finding the first-order solutions of the equations of motion, we first solve the RCE of first order. Given the exponential dependency of all the flow field variables on time via $exp(-\alpha_m t)$, we find for the extra-stress tensor of first order

$$\boldsymbol{\tau}_1 = 2\frac{1 - De_2\alpha_m}{1 - De_1\alpha_m}\boldsymbol{D}_1 =: 2\beta_1\boldsymbol{D}_1 . \tag{25}$$

This means that, at first order, the extra-stress tensor of the viscoelastic fluid differs from the Newtonian material just by a frequency-dependent factor β_1 in front of the rate-of-deformation tensor. This fluid is therefore formally identical to a Newtonian one, so that all the first-order results obtained in our previous paper [18] apply here, just with the Ohnesorge number Oh in those equations replaced by $Oh_v := \beta_1 Oh_0$. We therefore apply those previous results as follows.

Taking the curl of the first-order momentum equation in a vectorial form using equations (18) and (19), we obtain the fourth-order partial differential equation

$$\left(\frac{1}{Oh_v}\frac{\partial}{\partial t} - E_s^2\right)\left(E_s^2\psi\right) = 0 \quad \text{with} \quad E_s^2 = \frac{\partial^2}{\partial r^2} + \frac{\sin\theta}{r^2}\frac{\partial}{\partial\theta}\left(\frac{1}{\sin\theta}\frac{\partial}{\partial\theta}\right) , \tag{26}$$

which is the operator for the streamfunction [3]. The resulting streamfunction ψ consists of two contributions $\psi_1 + \psi_2$ [15] represented by the proportionalities

$$\psi_1 = C_{1m} r^{m+1} \sin^2\theta P'_m(\cos\theta) e^{-\alpha_m t} \quad \text{and} \quad \psi_2 = C_{2m} q r j_m(qr) \sin^2\theta P'_m(\cos\theta) e^{-\alpha_m t} \,, \tag{27}$$

where $P'_m(\cos\theta)$ is the first-order derivative of the Legendre polynomial P_m with respect to its argument and j_m is a spherical Bessel function of the first kind and order m. In its argument we have defined $q = \sqrt{\alpha_m / Oh_v}$. The radial and angular components of the first-order velocity vector follow as derivatives of the stream function

$$u_{r1} = -\left[C_{1m} r^{m-1} + C_{2m} q^2 \frac{j_m(qr)}{qr} \right] m(m+1) P_m(\cos\theta) e^{-\alpha_m t} \,, \tag{28}$$

and

$$u_{\theta 1} = \left[C_{1m}(m+1) r^{m-1} + C_{2m} q^2 \left((m+1)\frac{j_m(qr)}{qr} - j_{m+1}(qr) \right) \right] \sin\theta P'_m(\cos\theta) e^{-\alpha_m t} \,, \tag{29}$$

respectively. The two integration constants C_{1m} and C_{2m} are determined by the first-order kinematic and zero shear stress boundary conditions and read

$$C_{1m} = \frac{\hat{\eta}_1 \alpha_m}{m(m+1)} \left[1 + \frac{2\left(m^2-1\right)}{2q j_{m+1}(q)/j_m(q) - q^2} \right] \qquad C_{2m} = -\frac{2(m-1)\hat{\eta}_1 \alpha_m}{mq[2q j_{m+1}(q) - q^2 j_m(q)]}. \tag{30}$$

The first-order pressure field is obtained by integration of one component of the momentum equation as

$$p_1 = -C_{1m}(m+1)\alpha_m r^m P_m(\cos\theta) e^{-\alpha_m t} \,. \tag{31}$$

With the velocity and pressure fields known, the zero normal stress boundary condition of first order (21) yields the characteristic equation of the drop, which reads

$$\frac{\alpha_{m,0}^2}{\alpha_m^2} = \frac{2(m^2-1)}{q^2 - 2q j_{m+1}/j_m} - 1 + \frac{2m(m-1)}{q^2} \left[1 + \frac{2(m+1) j_{m+1}/j_m}{2 j_{m+1}/j_m - q} \right] \,, \tag{32}$$

This equation determines the complex angular frequency α_m, where we have denoted $\alpha_{m,0} = [m(m-1)(m+2)]^{1/2}$. The spherical Bessel functions are taken at the value q of their arguments. The equation is identical to the results from [2] and [5]. In the next section, we analyze solutions of the characteristic equation and compare them with experimental data.

Results of the Characteristic Equation and Discussion

There is an infinite manifold of solutions of the characteristic equation of a viscoelastic drop for a given range of Ohnesorge numbers and fixed Deborah numbers [2, 5]. We use aqueous solutions of the polyacrylamide Praestol 2500 and measure droplet oscillations using an ultrasonic resonator for levitating single drops [2]. Measured liquid drop properties for different solute mass fractions (SMF) are given in table 1. Due to the small solute contents, the density ρ for all solute mass factions equals 1000 kg/m^3. We use measured surface tension σ, droplet radius a, stress relaxation time λ_1 and deformation retardation time λ_2 from table 1 and the density to compute the Deborah numbers. For the SMF of 0.1 wt% and 0.5 wt%, the values of De_1

Table 1. Measured properties of the aqueous Praestol 2500 solutions and measured drop radius.

SMF [wt%]	μ_0 [Pa s]	λ_1 [s]	λ_2 [s]	σ [N/m]	a [m]
0.1	0.017	0.033	$0.396 \cdot 10^{-4}$	0.072	$1.067 \cdot 10^{-3}$
0.5	0.35	0.14	$0.189 \cdot 10^{-3}$	0.074	$1.08 \cdot 10^{-3}$

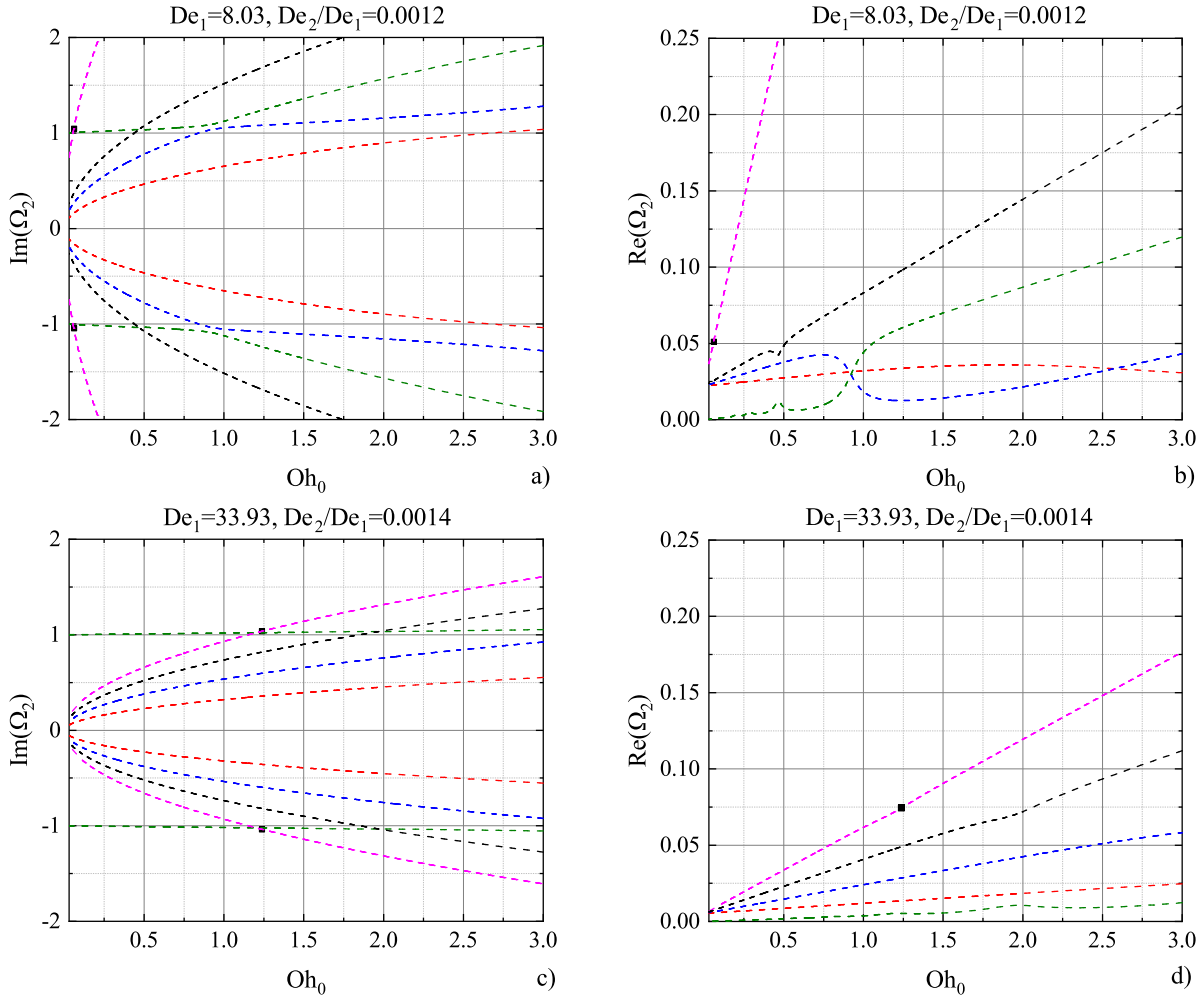

Figure 2. Solutions of the characteristic equation for polymer mass factions of 0.1 wt% (a and b) and 0.5 wt% (c and d), varying the Ohnesorge number. a) and c) - imaginary and b) and d) - real part of the nondimensional frequency Ω_2.

are 8.03 and 33.93, respectively. The values of De_2 are represented by the ratios of Deborah numbers in figure 2. The solutions of the characteristic equation are defined as nondimensional complex angular frequencies Ω_m, which are ratios of α_m and $\alpha_{m,0}$. The imaginary and the real parts of the complex angular frequency present the frequency and the damping rate of the drop shape oscillation, respectively. They are shown in figure 2 for the fundamental initial deformation mode, the range of Ohnesorge numbers between 0.03 and 3, and SMF of 0.1 and 0.5 wt%. The solutions are shown with dashed lines. There is an infinite number of curves for the fixed Deborah numbers and the range of Ohnesorge numbers, but in figure 2 we show only the first five. Since the characteristic equation yields an infinite number of roots for fixed Deborah numbers, one must select solutions appropriate for representing the shape oscillations. We compare the solutions with experimental results. For the 0.1 wt% and 0.5 wt% aqueous Praestol 2500 solution drops in table 1, the measured frequencies are $f = 114.49$ Hz and $f = 113.12$ Hz, respectively, and the damping rates are $\alpha_{2,r} = 35.16\ s^{-1}$ and $\alpha_{2,r} = 51.02\ s^{-1}$, re-

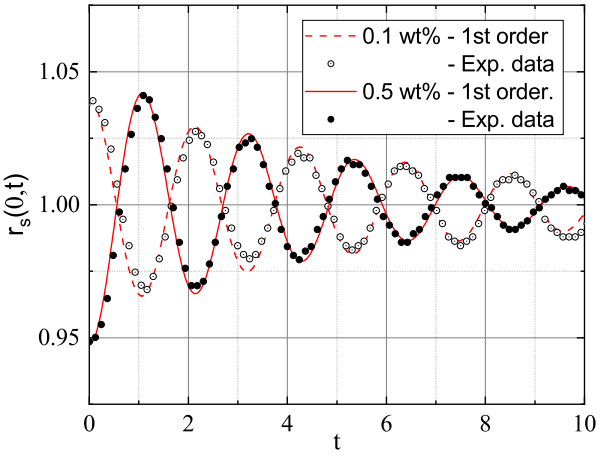

Figure 3. The trace of the drop north pole in time obtained from the linear solution and experimental data.

spectively. Therefore the complex angular frequencies $\alpha_2^* = \alpha_{2,r} + i2\pi f$ are known. The measured nondimensional complex angular frequency Ω_2 one formulates as $\alpha_2^*/\alpha_{2,0}^*$, where $\alpha_{2,0}^*$ is the dimensional Rayleigh frequency. The results with the corresponding Ohnesorge numbers are shown by the black squares in figure 2. The comparison yields perfect agreement between the measured and the calculated (pink dashed line) nondimensional complex angular frequencies. For drops with different Oh_0, but the same $m = 2$ and De_2/De_1, therefore, the values of Ω_2 can be taken from those lines. Figure 3 shows traces of the drop north pole obtained from the experiments and linear solutions using the first-order surface deformation (24). Frequency and damping rate of the linear solutions are known from the complex conjugate angular frequency for the corresponding liquid. The surface deformation amplitudes and phase angles are chosen according to the experimental data at $t = 0$. Length and time scale for the experimental data are nondimensionalized with the droplet radius and capillarity time scale, respectively. The theoretical and experimental data agree very well.

Conclusions

We derive the first-order solution with the characteristic equation for viscoelastic Oldroyd-B drop shape oscillations for use in the weakly nonlinear analysis. The characteristic equation yields an infinite number of solutions for the complex angular oscillation frequency. The appropriate solutions are selected according to experimental data for defining time dependencies in the higher-order solutions and the number of initial conditions in the analysis. The solutions of the characteristic equation agree well with the experimental data from damped drop shape oscillations of aqueous Praestol 2500 solution drops in an acoustic levitator. Since we select only one complex conjugate solution, the derivations of the second- and third-order equations and conditions together with their solutions are similar to the Newtonian case in [18].

Acknowledgements

This research was funded in whole by the Austrian Science Fund (FWF) I3326-N32. For the purpose of open access, the authors have applied a CC BY public copyright licence to any Author Accepted Manuscript version arising from this submission.

References

[1] Alonso, C. T., 1974, *Proc. of the Intern. Colloq. on Drops and Bubbles*, 1, pp. 139-157.
[2] Brenn, G., Plohl, G., 2015, *J. Non-Newton. Fluid Mech.*, 223, pp. 88-97.
[3] Bird, R.B. et al., 1962, 'Transport Phenomena', John Wiley & Sons, New York.
[4] Chandrasekhar, S., 1959, *Proc. London Math. Soc.*, s3-9, pp. 141-149.
[5] Khismatullin, D. B., Nadim, A., 2001, *Phys. Rev. E*, 63, p. 061508.
[6] Foote, G.B., 1973, *J. Comp. Phys.*, 11, pp. 507-530.
[7] Lamb, H., 1881, *Proc. London Math. Soc.*, s1-13, pp. 51-66.
[8] Lamb, H., 1932, 'Hydrodynamics', 6th ed. Cambridge University Press.
[9] Meradji, S. et at., 2001, *Cryst. Res. Technol.*, 36, pp. 729-744.
[10] Miller, C.A., Scriven, L.E., 1968, *J. Fluid Mech.*, 32, pp. 417-435.
[11] Prosperetti, A., 1980, *J. Fluid Mech.*, 100, pp. 333-347.
[12] Strutt, J.W., 1879, *Proc. R. Soc. London A*, 29, pp. 71-97.
[13] Renoult, M.-C. et al., 2018, *J. Fluid Mech.*, 856, pp. 169-201.
[14] Tsamopoulos, J.A., Brown, R.A., 1983, *J. Fluid Mech.*, 127, pp. 519-537.
[15] Tomotika, S., 1935, *Proc. R. Soc. London A*, 150, pp. 322-337.
[16] Trinh, E. H., Wang, T.G., 1982, *In Proc. 2nd Int. Colloq. on Drops and Bubbles*, pp. 82-87.
[17] Zrnić, D., Brenn, G., 2021, *J. Fluid Mech.*, A9.
[18] Zrnić, D., Berglez, P., Brenn, G., 2022, *Phys. Fluids*, 34(4), p. 043103.
[19] Zrnić, D., Brenn, G., 2022b, manuscript in preparation.